Modulated imaging: quantitative analysis and tomography of turbid media in the spatial-frequency domain

David J. Cuccia, Frederic Bevilacqua, Anthony J. Durkin, and Bruce J. Tromberg

Laser Microbeam and Medical Program, Beckman Laser Institute, University of California, Irvine, 1002 Health Sciences Road, Irvine, California 92612

Received November 1, 2004

Experiments performed on turbid phantoms demonstrate that spatially modulated illumination facilitates quantitative wide-field optical property mapping and tomographic imaging in turbid media. © 2005 Optical Society of America

OCIS codes: 170.3880, 170.5280, 170.6510, 280.0280.

We present a rapid, noncontact, scan-free method that facilitates wide-field optical property mapping and tomographic imaging in turbid media. The method is based on spatially modulated illumination, permitting sample characterization in the spatial-frequency domain. The advantage of such an illumination technique resides in the integration of optical property determination[1,2] and depth-resolved imaging of sample heterogeneity.

The spatial-frequency dependence of sample reflectance encodes both optical property and depth information. By introducing a spatially modulated source [Eq. (1)] into the steady-state diffusion equation [Eq. (2)],

$$S = S_0[1/2 + M \sin(2\pi f_x x)], \quad (1)$$

$$\nabla^2\phi - \mu_{\mathrm{eff}}^2\phi = S, \quad (2)$$

where $\mu_{\mathrm{eff}}=[3\mu_a(\mu_a+\mu_s')]^{1/2}$ and where $\delta_{\mathrm{eff}}=1/\mu_{\mathrm{eff}}$ is the effective penetration depth of the illumination, we arrive at the result

$$\partial_z{}^2\phi_{\mathrm{AC}} - \mu_{\mathrm{eff}}'^2\phi_{\mathrm{AC}} = MS_0, \quad (3)$$

$$\mu_{\mathrm{eff}}'^2 = \mu_{\mathrm{eff}}^2 + (2\pi f_x)^2. \quad (4)$$

Here S, M, and f_x are the illumination source, the modulation depth, and the spatial frequency (or repetition rate), respectively, Φ is the internal fluence rate, and Φ_{AC} refers to the harmonically varying component of the fluence rate. The spatially modulated wave propagates in turbid media as a planar illumination source S_0 would, except that the penetration depth, $1/\mu_{\mathrm{eff}}'$, depends on the spatial frequency of the illumination. The propagation of an arbitrary illumination function can be modeled through linear superposition of sinusoids in two directions. There are two major implications to Eqs. (3) and (4): First, by analyzing the frequency-dependent reflectance, one can quantitatively sample the optical properties of the medium. This method is analogous to the broadband frequency-domain photon migration approach,[3] for which time and spatial-frequency measurements are related by Fourier transformation to time-resolved and spatially resolved measurements, respectively. Second, varying the spatial frequency of the illumination pattern allows one to control the depth sensitivity of detection inside the turbid medium, whereas using planar illumination corresponds to a fixed mean depth of interrogation. Tomography in turbid media based on this principle has not yet been demonstrated to our knowledge. We demonstrate this technique within the context of diffusion theory but note that the qualitative behavior remains valid when the diffusion approximation fails, as demonstrated by Monte Carlo simulations.

Experimental data were acquired by use of a digital projector that employs a digital micromirror device (NEC HT1000) for illumination. Sinusoid patterns of various spatial frequencies in one direction are projected onto the sample of interest and captured by a Peltier-cooled 16-bit CCD camera (Roper Cascade 512F). Specular reflection is prevented by illumination at a small angle to normal incidence and by use of crossed linear polarizers. Interference filters permit selection of a narrow-wavelength band (shown here: $\lambda=640$ nm, $\Delta\lambda=20$ nm FWHM). A siloxane TiO_2 reflectance standard is used to calibrate the measured intensity and to correct for spatial nonuniformity in both the illuminating and imaging systems.

The illumination is in the form of Eq. (1), containing a dc (planar) component to allow for modulation from 0 to 1 ($M \sim 1$). To view the reflectance that is due to the ac and dc components separately, a phase shifting technique that is commonly used in communications systems is employed.[4] This sample is illuminated three times at the same spatial frequency, with phase offsets of 0, $2/3\ \pi$, and $4/3\ \pi$ rad. An image of the ac modulated reflectance is given by

$$\mathrm{ac} = (2^{1/2}/3)[(A-B)^2 + (B-C)^2 + (C-A)^2]^{1/2}, \quad (5)$$

where A, B, and C represent the reflectance images with shifted spatial phases. This simple pixel-by-pixel three-point amplitude demodulation technique was recently employed by Neil *et al.* for use in confocal microscopy.[5]

In a first set of experiments, we imaged a siloxane TiO_2 phantom designed to have homogeneously distributed optical properties. The bulk optical proper-

0146-9592/05/111354-3/$15.00

ties at 640 nm were $\mu_a = 0.0074\ \mathrm{mm}^{-1}$ and $\mu_s' = 0.90\ \mathrm{mm}^{-1}$, as measured by large source–detector separation frequency-domain photon migration.[3] Eleven three-image sets were acquired over a 5 cm $\times$ 5 cm surface, with spatial frequencies ranging from 0 to 0.6 mm^{-1}. Modulation images at each frequency were obtained as in Eq. (5). The resultant 11 images provide a quantitative frequency response, or modulation transfer function (MTF), of the diffuse reflectance of the turbid phantom. Moreover, this diffuse MTF is available at each pixel. One can predict diffuse reflectance relative to frequency analytically by taking a spatial Fourier transform of a spatially resolved reflectance model.[6] This facilitates the use of phantom-based calibration and least-squares regression to obtain the absolute optical properties of the sample.

Example MTF data are shown in Fig. 1 (open squares). Each data point represents an average over the entire modulation image. Notice that the tissue sample acts as a low-pass filter, attenuating the reflectance more strongly as spatial frequency increases. These data were fitted to an analytical diffuse reflectance model by use of a nonlinear least-squares optimization routine. The recovered μ_a and μ_s' optical properties of $\mu_a = 0.0080\ \mathrm{mm}^{-1}$ and $\mu_s' = 0.97\ \mathrm{mm}^{-1}$ show agreement within 10% with the bulk frequency-domain photon migration values. A separate MTF at each pixel facilitates optical property imaging. This imaging was performed over the 5 cm $\times$ 5 cm area (approximately 500 pixels $\times$500 pixels). Maps of the recovered absorption and scattering properties are shown in Fig. 2, demonstrating small spatial variations in the phantom optical properties. To the right of each map is a histogram of pixel values, with a dashed line indicating the known bulk value. The recovered properties are in good agreement with the known average bulk properties, with the bulk properties falling well within the corresponding histograms. Previous approaches have reported only average optical property determination by use of periodic illumination.[2] To our knowledge this is the first report of wide-field imaging of quantitative optical properties in the spatial-frequency domain.

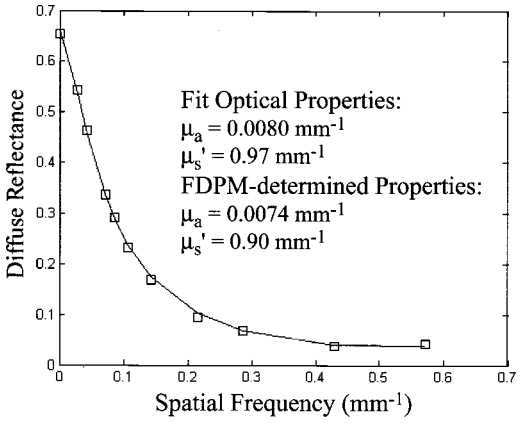

Fig. 1. Example multifrequency data (open squares) and corresponding fit (solid curve). The turbid medium acts as a low-pass filter.

In a second set of experiments, a siloxane TiO_2 standard ($\mu_a = 0.003\ \mathrm{mm}^{-1}$ and $\mu_s' = 1\ \mathrm{mm}^{-1}$ at 640 nm) was modified to accommodate two heterogeneities, shown in Fig. 3. The first object, a 2 mm-thick absorbing mask (triangular in shape), was placed 2 mm inside the sample. The second heterogeniety was a 1-mm-thick scattering and absorbing element (square in shape) placed at the surface of the siloxane block (thickness, 0.5 mm; $\mu_a = 0.006\ \mathrm{mm}^{-1}$; $\mu_s' = 1\ \mathrm{mm}^{-1}$).

Modulation images at 42 spatial frequencies were acquired, ranging from 0 to 0.63 mm^{-1}. Figure 4 illustrates data acquired at 0, 1, 4, and 30 times a sampling frequency of 0.0191 mm^{-1}. Listed above each image are the spatial frequency, f_x, and the corresponding diffuse penetration depth for the homogeneous background property, δ_h. The top row of figures contains sample raw reflectance images at these illumination frequencies, where each image contains both a modulated (ac) and a planar (dc) term. Note the apparent spatial distortion of the waves, a consequence of the strong ac signal demodulation in these regions compared with the dc component. The middle row is the resulting ac modulation image at each corresponding frequency, calculated from Eq. (5). For fair comparison, each image is plotted within 0.5 and 1.5 times its average pixel value.

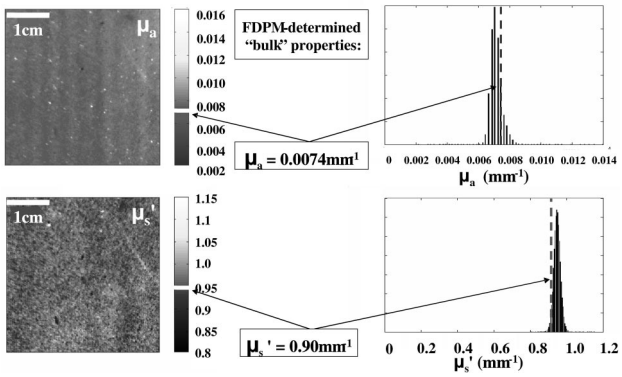

Fig. 2. Absorption (top) and scattering (bottom) data of the spatially varying phantom optical properties. Quantitative images (inverse millimeters, left) and corresponding pixel histograms (right) demonstrate good agreement with known bulk properties.

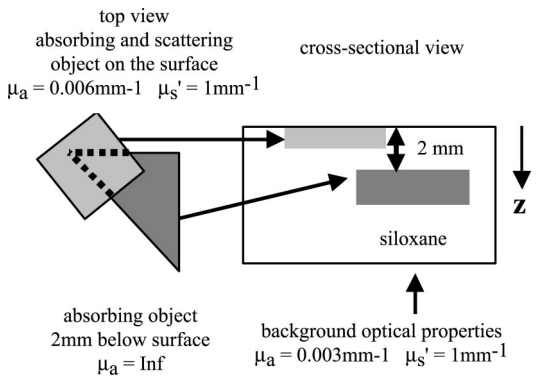

Fig. 3. Schematic diagram of a heterogeneous phantom.

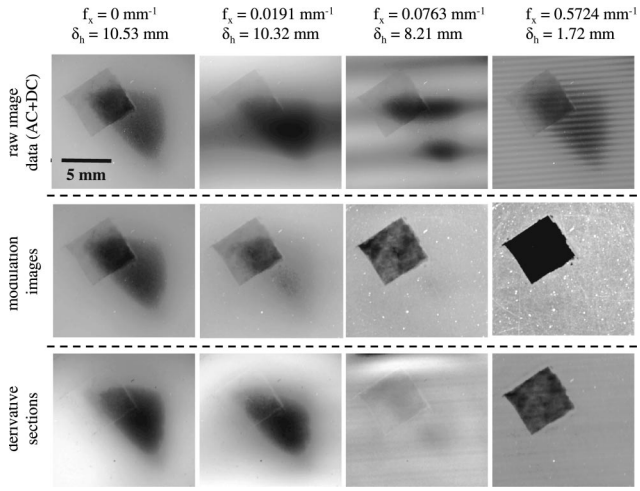

Fig. 4. Top to bottom, raw reflectance, ac modulation, and frequency-derivative images of the heterogeneous phantom.

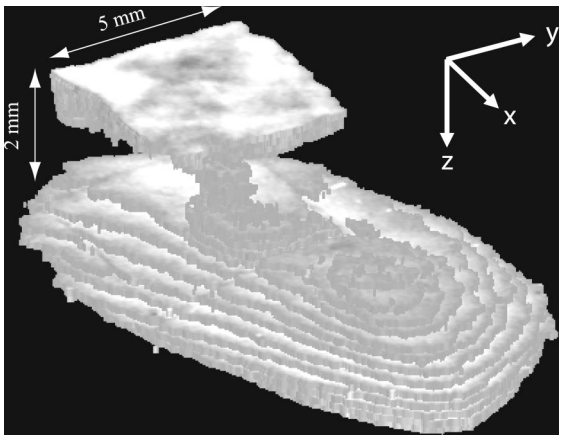

Fig. 5. Optical tomograph of the heterogeneous turbid phantom from frequency-derivative images.

The effective contrast of the different objects depends on the spatial frequency of the illumination. In the dc modulation image (Fig. 4, middle, left), both superficial and deep objects appear. However, as the spatial frequency of illumination increases (to the right), the lower object becomes decreasingly apparent, until finally only the superficial object is visible. This result is consistent with our theoretical formulation, which predicts that high-frequency photon density waves penetrate only superficially.

Encoded in the modulation data are depth-resolved optical properties. A range of quantitative tomographic reconstruction techniques for turbid media can be applied toward solving the spatially heterogeneous inverse problem in three dimensions.[7] Nevertheless, a simple numerical derivative of modulation with frequency permits visualization of the change in depth contrast versus frequency. The bottom row of Fig. 4 illustrates this with a derivative image calculated at each of the four example sampling frequencies by use of a Savitzky–Golay differentiation filter. Notice that changes at low and high frequencies are exclusively sensitive to the lower and upper objects, respectively. Note also that the lowest-contrast derivative image (bottom, third figure from left), corresponds to the gap between the two heterogeneities. This method therefore facilitates tomographic imaging in large turbid volumes with wide fields of view. In Fig. 5 we show a three-dimensional tomographic rendering of the derivative data set. A single thresholding was performed, and the slice thicknesses were weighted to correspond to the appropriate penetration depths. The depth scale was marked from *a priori* knowledge of the phantom dimensions. The two objects are clearly resolved, with resolution appearing to degrade with depth. Quantitative reconstruction, aided by the robust measure of the sample's average MTF and thus average optical properties,[7] is expected to compensate partially for this effect and to provide quantitative depth information.

In conclusion, we have demonstrated a rapid and potentially inexpensive procedure for achieving tomography and quantitative optical property mapping in turbid media over wide fields of view. We are currently conducting contrast-to-background sensitivity analyses for more challenging perturbations as well as for characterizing the quantitative capability of the technique across a broad range of optical properties. We expect that this technique will develop to fill the gap in biological tissue imaging between submillimeter imaging techniques (confocal–multiphoton microscopy, optical coherence tomography) and diffuse optical tomography.

This research was supported by the National Institutes of Health under grant RR01192 (Laser Microbeam and Medical Program). Programming support from the Beckman Foundation and the U.S. Air Force Office of Scientific Research is gratefully acknowledged. D. J. Cuccia's e-mail address is dcuccia @uci.edu.

References

1. F. Bevilacqua, D. Piguet, P. Marquet, J. Gross, B. Tromberg, and C. Depeursinge, Appl. Opt. **38**, 4939 (1999).
2. N. Dognitz and G. Wagnieres, Lasers Med. Sci. **13**, 55 (1998).
3. T. Pham, O. Coquoz, J. Fishkin, E. Anderson, and B. J. Tromberg, Rev. Sci. Instrum. **7**, 2500 (2000).
4. A. B. Carlson, *Communication Systems* (McGraw-Hill, New York, 1988).
5. M. A. A. Neil, R. Juskaitis, and T. Wilson, Opt. Lett. **22**, 19057 (1997).
6. A. Kienle, L. Lilge, M. S. Patterson, R. Hibst, R. Steiner, and B. C. Wilson, Appl. Opt. **35**, 2304 (1996).
7. X. Cheng and D. A. Boas, Opt. Express **3**, 118 (1998), http://www.opticsexpress.org.